Published in final edited form as:
Cancer Res. 2012 March 1; 72(5): 1103–1115. doi:10.1158/0008-5472.CAN-11-3380.

VEGF receptor inhibitors block the ability of metronomically dosed cyclophosphamide to activate innate immunity-induced tumor regression

Joshua C. Doloff and **David J. Waxman***
Division of Cell and Molecular Biology, Dept. of Biology, Boston University, Boston, MA 02215 USA

Abstract

In metronomic chemotherapy, frequent drug administration at lower than maximally tolerated doses can improve activity while reducing the dose-limiting toxicity of conventional dosing schedules. Although the anti-tumor activity produced by metronomic chemotherapy is attributed widely to anti-angiogenesis, the significance of this mechanism remains somewhat unclear. In this study, we show that a 6-day repeating metronomic schedule of cyclophosphamide administration activates a potent antitumor immune response associated with brain tumor recruitment of natural killer (NK) cells, macrophages, and dendritic cells that leads to tumor regression. Tumor regression was blocked in NOD-scid-gamma mice, which are deficient or dysfunctional in all these immune cell types. Furthermore, regression was blunted by NK cell depletion in immune competent syngeneic mice or in perforin deficient mice, which are compromised for NK, NKT, and T cell cytolytic functions. Unexpectedly, we found that VEGF receptor inhibitors blocked both innate immune cell recruitment and the associated tumor regression response. Cyclophosphamide administered at a maximum-tolerated dose activated a transient, weak innate immune response, arguing that persistent drug-induced cytotoxic damage or associated cytokine and chemokine responses are required for effective innate immune-based tumor regression. Together, our results reveal an innate immune-based mechanism of tumor regression that can be activated by a traditional cytotoxic chemotherapy administered on a metronomic schedule. These findings suggest the need to carefully evaluate the clinical effects of combination chemotherapies that incorporate anti-angiogenesis drugs targeting VEGF receptor.

Keywords

Metronomic chemotherapy; Innate Immunity; Tumor Regression

Introduction

Maximum-tolerated dose (MTD) chemotherapy has been a mainstay in the cancer clinic for the past 50 years. However, recent preclinical successes with metronomic chemotherapy, where drug is administered at a regular, more frequent interval, but at a lower dose than MTD chemotherapy, have been rapidly translated into clinical trials, where improved anti-tumor responses have been observed (1). Metronomic chemotherapy eliminates the need for extended recovery periods between treatment cycles and thus allows for persistent drug treatment in a way that minimizes drug toxicity to the patient (2). Metronomic

*To whom correspondence should be addressed: Dr. David J. Waxman, Department of Biology, Boston University, 5 Cummington Street, Boston, MA 02215 USA, djw@bu.edu.

chemotherapy schedules using cyclophosphamide (CPA) and other chemotherapeutic drugs induce endothelial cell death in addition to tumor cell death (2–4). Metronomic chemotherapy also induces the anti-angiogenic glycoprotein thrombospondin-1 (TSP1; *Thbs1*) (4,5), suggesting that anti-angiogenesis is an important factor in the superior anti-tumor profiles of metronomic regimens (6,7). However, this proposed mechanism is not supported by the finding that *bona fide* anti-angiogenic drugs often show only moderate anti-tumor activity when used as single agents, despite their effectiveness at inhibiting tumor angiogenesis. Examples of this include non-small cell lung cancer (8) and glioblastomas (9) in human patients, 9L gliosarcoma xenografts treated in *scid* mice (4), and metastatic melanomas in C57BL/6 mice (10). Thus, other mechanisms for the improved anti-tumor effects of metronomic chemotherapy are likely operative.

TSP1, in addition to its anti-angiogenic activity, has other actions, including stimulation of chemotaxis, cell proliferation, and protease regulation in healing (11). Moreover, tumors that stably express TSP1 have significantly increased levels of infiltrating anti-tumor M1 macrophages (12), suggesting a role for the host immune system in the improved tumor responses to metronomic drug treatments.

Presently, we show that a 6-day repeating metronomic schedule of CPA activates a potent and sustained anti-tumor innate immune response that is associated with tumor regression and leads to ablation of large brain tumor xenografts. In contrast, MTD CPA treatment induces a weak immune response that dissipates during the rest period between treatment cycles. We further demonstrate that anti-tumor innate immunity, and not anti-angiogenesis, is the major mechanism for the marked tumor regression seen in these models. Supporting this hypothesis, tumor regression is blocked in NK cell-deficient and macrophage and dendritic cell-dysfunctional NOD-scid-gamma mice (13), and is blunted by NK cell-depletion in an immune competent syngeneic mouse model, and in mice deficient in the lymphocyte effector molecule perforin, where NK, NKT, and T cell cytolytic function are compromised (14).

In addition, we show that VEGF receptor-selective anti-angiogenic drugs block anti-tumor immunity and prevent metronomic CPA-induced tumor regression. VEGF receptor signaling is important for dendritic cell-endothelial cell cross-talk, trans-differentiation (15), tumor-associated macrophage infiltration (16), and chemokine expression and secretion in proinflammatory responses (17). Furthermore, endothelial cells and immune cells have shared bone marrow-derived stem and progenitor cells regulated by VEGF receptor (18), suggesting that compounds designed to kill tumor blood vessels by inhibiting VEGF receptor signaling may also elicit immune suppressive responses.

Materials and Methods

Cell lines

Human U251 glioblastoma cells (NCI, Bethesda, MD), rat 9L gliosarcoma cells (Neurosurgery Tissue Bank, UCSF, San Francisco) and mouse GL261 glioma cells (DCTD, DTP Tumor Repository, Frederick, MD) were authenticated by and obtained from the indicated sources. Cells were grown at 37°C in a humidified, 5%CO_2 atmosphere. U251 and GL261 cells were grown in RPMI-1640 and 9L in DMEM medium, all of which contained 10% FBS, 100Units/ml penicillin and 100μg/ml streptomycin.

Mouse models and tumor xenografts

Five-wk-old (24–26g) male ICR/Fox Chase immune deficient *scid* mice (Taconic Farms, Germantown, NY), 5-wk-old male NOD.Cg-*Prkdc*^{scid} *Il2rg*^{tm1Wjl}/SzJ (NOD-scid-gamma, NSG) mice (Jackson Labs, Bar Harbor, ME), and 5-wk-old (22–24g) male C57BL/6 (wild-

type (WT), immune competent) (Taconic) and C57BL/6-Prf1^{-} (perforin knock-out) (Jackson Labs) mice were housed and treated under approved protocols and federal guidelines. Tumor cells (2×10^6 GL261 glioma cells, 4×10^6 9L cells, or 6×10^6 U251 glioblastoma cells) were injected *s.c.* on each posterior flank in 0.2ml serum-free RPMI using a 0.5-inch 29-gauge needle and a 1ml insulin syringe. 9L and U251 tumor xenografts were grown s.c. on the flanks of *scid* or NSG mice, and GL261 tumors were inoculated into the flanks of C57BL/6 (WT or Prf1^{-}) mice. Tumor areas (length × width) were measured twice weekly using Vernier calipers (VWR, Cat#62379-531) and tumor volumes were calculated based on the formula $Vol=(\pi/6)*(L*W)^{3/2}$. Tumors were monitored and treatment groups were normalized (each tumor volume set to 100%) once average tumor volumes reached $500mm^3$. Mice were treated with CPA given on an intermittent metronomic schedule (140mg CPA/kg-body weight (BW), repeated every 6-days) or on an MTD schedule (150mg CPA/kg-BW on each of two consecutive days, followed by a 19d rest period) as indicated on each Figure using vertical arrows. Axitinib (Ax) and AG-028262 were administered daily at 25mg/kg-BW/day i.p. and cediranib (AZD) at 5mg/kg-BW/day i.p. for up to 24d, as indicated in each study. NK cell-depleting monoclonal antibody anti-asialo-GM1 (cat.#986–10001, Wako Chemicals USA, Richmond, VA) was administered i.p. at a dose of 50μl (diluted 1:3 in sterile 1xPBS to 150μl final volume for each mouse on the day of injection) and delivered once every 6d starting 3d prior to the first metronomic CPA treatment (i.e., asialo-GM1 antibody was given 3d prior to each CPA injection). On combination therapy days, CPA was administered 4h prior to treatment with a VEGF receptor inhibitor to minimize the potential for drug interactions. Tumor sizes and mouse body weights were measured at least twice a week. Tumor growth rates prior to drug treatment were similar among all normalized groups.

qPCR and statistical analysis

RNA isolation, qPCR primer design and qPCR analyses as described in Supplementary Materials and Methods. qPCR data are expressed as mean values ±S.E. for n=5–6 individual tumors from 3 mice/time point/treatment group unless indicated otherwise. Statistically significant differences between mean values of different treatment groups were determined by two-tailed Student's t-test; *, $p<0.05$; **, $p<0.001$; and ***, $p<0.0001$.

Other methods

Sources of reagents and drugs, FACS analysis and immunohistochemical methods are described in Supplementary Materials and Methods.

Results

Metronomic CPA-induced regression of brain tumor xenografts does not involve anti-angiogenesis

Although anti-angiogenesis is considered a key mechanistic feature of metronomic chemotherapy, metronomic CPA treatment of *scid* mice bearing U251 glioblastoma xenografts induces tumor regression that is sustained and complete (Fig.1A) in the absence of anti-angiogenesis (Fig.1B). In contrast, the VEGF receptor-selective inhibitor axitinib (19) is strongly anti-angiogenic (Fig.1B) yet primarily shows a growth static response, followed by rapid tumor regrowth upon discontinuation of treatment (Fig.1A). Axitinib initially increased anti-tumor activity when combined with metronomic CPA treatment, but ultimately blocked the tumor regression seen with metronomic therapy alone. Partial tumor regression was eventually seen after discontinuation of axitinib treatment, followed by rapid tumor regrowth after termination of metronomic chemotherapy. An initial improvement in tumor response followed by inhibition of metronomic CPA-induced tumor regression was also observed with axitinib co-treatment in the 9L gliosarcoma model (4).

Metronomic CPA activates anti-tumor innate immunity

To better understand why metronomic CPA fully regresses U251 tumors, even in the absence of anti-angiogenesis, we investigated other potential mechanisms and found that several macrophage-associated host factors are increased in the metronomic CPA-treated tumors, including TSP1 (Fig.1C). While TSP1 has anti-angiogenic activity (5), it has also been linked to tumor infiltration by anti-tumor M1 macrophages (12). Metronomic CPA also increased host (mouse cell) expression of PEDF (pigment epithelium-derived factor; *Serpinf1*) (Fig.1D), an anti-angiogenic factor that also stimulates M1 macrophage recruitment to tumors (20). These responses were seen in both rat 9L and human U251 tumors grown in *scid* mice, where TSP1 and PEDF levels were strongly correlated (r=0.89) in large sets of untreated and drug-treated tumors isolated various times after initiation of metronomic CPA treatment (Fig.S1). Metronomic CPA also induced the host macrophage markers CD68 and F4/80 (Fig.2A; Fig.S2A), macrophage cytolyic effector lysozymes 1 and 2 (Fig.S2B), and the death receptor Fas (Fig.2B), which activates macrophages and increases their tumor cytotoxicity (21).

The above findings suggested that metronomic CPA activates an innate immune response in the regressing tumors. To investigate this possibility, we considered natural killer (NK) cells, given the role of Fas in mediating interactions between NK cells and cells marked for destruction (22). In metronomic CPA-treated tumors, we observed large increases in the host NK cell marker NK1.1 and in the NK cell-associated cytotoxic granzymes A, B and C and perforin (Figs. 2A and 2C; Figs. S2C and S3A–S3C), which are essential for cytotoxic lymphocyte-mediated cell death (22). FACS analysis confirmed the influx of $NK1.1^+$ cells into the metronomic CPA-treated tumors (Fig.2D; Fig.S3D). Dendritic cells were also recruited to the tumors, as shown by the activation of host dendritic cell markers important for cell-target interactions and antigen presentation to the adaptive immune system (Fig.2E). CD74, implicated in the regulation of dendritic cell migration (23), was also increased (Fig. 2A; Figs. S2D, S3A,B). Since NK1.1 and dendritic cell markers are both increased in the CPA-treated tumors, other $NK1.1^+$ cells, such as interferon-producing killer dendritic cells (24), could also be involved. Host cytokine and chemokine immune attractants, such as IL-12β and CXCL14, which can influence leukocyte and lymphocyte activation and migration (25), were also increased in the metronomic CPA-treated U251 and 9L tumors (Figs. 3A and 3B), suggesting their role in mobilizing the host innate immune response.

VEGF receptor-targeted inhibitors block metronomic CPA-activated anti-tumor immunity

We next sought to determine why the VEGF receptor inhibitor axitinib blocks tumor regression induced by metronomic CPA treatment (4). In both U251 and 9L tumors, axitinib blocked tumor infiltration of NK cells, macrophages and dendritic cells (Fig.2, Figs. S2, S3A–S3C). Axitinib also blocked the formation of chemokine and cytokine gradients that may mobilize these cells into tumors (Fig.3A, 3B). Importantly, axitinib suppressed these immune factors to basal, or below basal levels. Axitinib also suppressed the induction by metronomic CPA of human tumor cell-expressed MICB (Fig.3C), which is an activating ligand for the receptor NKG2D found on NK and other immune cells (26). This finding suggests that axitinib might further inhibit metronomic CPA-induced tumor cell-targeted anti-tumor immunity by blocking the expression and subsequent presentation of activation signals by CPA-damaged tumor cells. Finally, axitinib shifted the balance of tumor-associated macrophages from anti-tumor M1 (marked by iNOS) to pro-tumor M2 macrophages (marked by arginase-1) (Fig.3D). Thus, the inhibitory effects of axitinib on metronomic CPA-induced tumor regression likely result from interference with the innate immune response at multiple levels.

Next, we used two other anti-angiogenic tyrosine kinase inhibitors, cediranib (AZD2171) (27) and AG-028262 (28), to investigate the importance of VEGF receptor signaling for metronomic CPA-induced anti-tumor immunity. These two chemicals exhibit selectivity for VEGF receptor inhibition comparable to or greater than that of axitinib (27,28). In U251 tumors grown in *scid* mice, cediranib and AG-028262 strongly inhibited tumor angiogenesis, as expected (Fig.4A); however, they also blocked metronomic CPA-induced NK cell activity (Fig.4B) and the recruitment of all three classes of innate immune cells (Fig.4C). Moreover, by the sixth day of treatment, both drugs blocked U251 regression induced by metronomic CPA, resulting in tumor growth stasis that continued until the study was terminated on treatment day 18; whereas, over that same time period, tumors treated with metronomic CPA alone regressed a further 50% in volume. Thus, interference with metronomic chemotherapy-induced anti-tumor immunity and tumor regression are general responses to VEGF receptor inhibitors.

Metronomic CPA-induced tumor regression requires innate immune cells

To test whether the tumor-infiltrating innate immune cells contribute functionally to tumor regression, we investigated the effects of metronomic CPA treatment on 9L gliosarcomas grown in NOD-*scid*-IL2Rγ-null (NSG) mice, which, unlike *scid* mice, are NK cell deficient and have dysfunctional macrophages and dendritic cells due to loss of the important immunostimulatory interleukin-2Rγ receptor (13). In NSG mice, metronomic CPA-induced 9L tumor growth delay led to growth stasis after several treatment cycles but no regression (Fig.5A). While macrophages, dendritic cells, and markers for other innate immune cell types such as neutrophils and platelets are present in the tumors and are increased by metronomic CPA (Figs. 5B and 5C), NK cells (NKp46) and their cytotoxic effectors, granzyme B (GzmB) and perforin (Prf1), were undetectable (Fig.5C). Thus, the large differential anti-tumor response between NSG mice (tumor growth stasis) and *scid* mice (full tumor regression) (Fig.5A) can be attributed to the diminished innate immune response to metronomic CPA in NSG mice (Fig.5C, left: NSG vs. *scid*). NK cell factors (NKp46, NK1.1, GzmB, and Prf1) were also deficient in spleen in both untreated and CPA-treated NSG spleens as compared to *scid* mice (Fig.5C, right: NSG vs. *scid*), as expected. Progressive depletion of NK cells from *scid* mouse splenic reservoirs with continued metronomic CPA treatment was also apparent (Fig.5C, *right*). The tumor growth stasis seen in NSG mice likely reflects residual anti-tumor immune cell responses (Figs. 5B and 5C) and the intrinsic cytotoxicity of CPA towards tumor cells and tumor endothelial cells. The delayed increase in the NK cell markers NKp46 and perforin in CPA-treated *scid* mouse 9L tumors (Fig.5C) is consistent with the delayed onset of tumor regression (Fig.5A), further implicating NK cell function in this response to metronomic CPA. Finally, a strong increase in TSP1 expression was seen in the metronomic CPA-treated NSG mouse 9L tumors (Fig. 5B), despite the lack of tumor regression. Thus, TSP1 and its anti-angiogenic activity are not sufficient to drive tumor regression, which may help explain why TSP1 production is not a reliable marker for clinical response to metronomic chemotherapy (29).

Metronomic CPA-activated anti-tumor immunity and tumor regression in an immune competent, syngeneic mouse model

To ascertain whether the strong innate immune responses to metronomic CPA treatment are limited to animals with deficiencies in T- and B-adaptive immune cells, the impact of metronomic CPA was investigated in immune competent C57BL/6 mice bearing the syngeneic glioma GL261. These studies additionally enabled us to determine whether metronomic CPA activates a T- or B-cell adaptive immune response, and whether regulatory suppressor T cells (Tregs) are also recruited to the tumors, and might interfere with anti-tumor immunity (30). Strikingly, metronomic CPA fully regressed all GL261 tumors (Table S1), with no tumor regrowth seen at day-140, i.e., 80-days after halting metronomic CPA

(Fig.6A; WT CPA, *solid diamond*). Large increases in tumor-associated NK cells, dendritic cells, and macrophages occurred at the onset of tumor regression and continued for at least 4 metronomic CPA cycles (Fig.6B, *left*). We also observed delayed recruitment of $CD4^+$ helper T-cells and $CD8^+$ cytotoxic T-effector cells to the regressing tumors, but no increase in Tregs (marked by FoxP3) (Fig.6B, *right*). The latter finding is consistent with the reported selectivity of metronomic CPA for killing Tregs but not cytotoxic anti-tumor T-effector cells (30,31).

Causal role for innate immune cells in tumor regression

The functional consequence of NK cell recruitment was probed by NK cell depletion using anti-asialo-GM1 antibody (32), which resulted in delayed and substantially incomplete GL261 tumor regression (Fig.6A, open triangle; Table S1). Tumor cell recruitment of NK cells was fully blocked by asialo-GM1 antibody over multiple CPA treatment cycles, and splenic NK cell levels were also suppressed (Fig.6C, *top*). Metronomic CPA recruitment of dendritic cells and macrophages was unaffected by NK cell depletion (Fig.6C, *bottom*) and may contribute to the partial tumor regression observed. Importantly, NK cell recruitment and complete tumor regression were both restored following termination of asialo-GM1 antibody treatment on day-51 (Fig.6A, open triangles). Thus, while other immune cells likely contribute to metronomic CPA-induced tumor regression, NK cells are required both for the early onset and for the completeness of tumor regression. Metronomic CPA-induced GL261 regression was also delayed and even less complete in C57BL/6 mice deficient in perforin (Fig.6A, solid squares; Table S1). Perforin deficiency severely decreases not only NK cell, but also NKT cell and cytotoxic T-cell cytolytic activity (14). The further diminished anti-tumor response in the perforin-knockout mice suggests that adaptive immune lymphocytes contribute to tumor regression. Markers for host adaptive immune $CD8^+$ T-lymphocytes and innate immune NK cells, macrophages, and dendritic cells were all strongly induced in GL261 tumors by metronomic CPA-treatment of the perforin knockout mice (Fig.S4A). Thus, despite intact immune cell mobilization, the impairment of lymphocyte cytolytic function in the absence of perforin is sufficient to seriously impair metronomic CPA-induced tumor regression. Thus, the host immune system is essential for metronomic CPA-induced tumor regression.

MTD CPA induces a weak, transient innate immune response

U251 tumors grown in *scid* mice initially responded to MTD CPA treatment, however, the response was short-lived and was followed by resumption of rapid growth during the drug-free recovery period between treatment cycles (Fig.7A). An initial, modest innate immune response to MTD CPA dissipated during the recovery period, whereas the response to metronomic CPA was sustained and became maximal by day-18, as judged by the increased expression of the cytotoxic effector granzyme B (Fig.7B, *top*) and other immune cell markers (Fig.7C). MTD CPA treatment did increase overall granzyme B exposure, by ~ 40%; however, the increase following metronomic CPA treatment was >10-fold higher (Fig. 7B, *bottom*).

Discussion

The present findings identify innate immune cell recruitment, and not TSP1-mediated anti-angiogenesis, as a major, functionally important mechanism for the dramatic regression of brain tumor xenografts treated with CPA on a 6-day repeating, metronomic schedule. This immune response involves a strong NK cell component that contributes functionally to tumor regression. These findings are based on studies in three brain tumor models, including a syngeneic, fully immune competent mouse model, indicating it is not due to immune dysregulation as a result of the lack of an adaptive immune system. In contrast, MTD CPA

did not induce immune recruitment leading to tumor regression, indicating that the scheduling of chemotherapy is a critical requirement for this innate immune response. Finally, several VEGF receptor-selective anti-angiogenesis drugs were shown to block innate immune recruitment, implicating VEGF receptor in the mechanism whereby metronomic CPA activates innate immunity. The latter finding is particularly important given the widespread efforts to develop effective ways to combine VEGF receptor inhibitors with traditional cytotoxic anti-cancer drugs.

Metronomic CPA-induced tumor infiltration by macrophages, dendritic cells and NK cells was established using both structural and functional markers for each immune cell type. In the case of NK cells, strong induction of several functional markers was observed, notably NKp46, perforin, and granzymes A, B and C. Moreover, functionality was *de facto* established by GM1 antibody depletion, which seriously compromised metronomic CPA-induced tumor ablation, with tumor regression resuming shortly after antibody depletion was terminated. Functional markers for the tumor-recruited macrophages included the macrophage cytolytic effectors lysozyme 1 and lysozyme 2, which showed large increases in the treated tumors, and in the case of dendritic cells, DC-SIGN (CD209), which is important for dendritic cell function and antigen presentation. The increases in DC-SIGN exceeded those of the dendritic cell structural markers CD207 (Langerin) and CD74, suggesting an increase in dendritic cell activity in addition to recruitment in response to metronomic CPA treatment. Markers for other innate immune cells, such as platelets and neutrophils, were also increased, however, further studies will be required to fully characterize their involvement in metronomic CPA-activated anti-tumor immunity and tumor regression.

Conceivably, other cytotoxic chemotherapeutic drugs may also induce a sustained anti-tumor innate immune response when given on a metronomic schedule (1). Metronomic chemotherapies may thus complement strategies to counter immune evasion by tumor cells, such as *ex vivo* immune cell augmentation, host immune ablation and adoptive immunotherapy (33). In other studies, low-dose chemotherapy can modulate various anti-tumor immune responses. Examples include the ability of vinblastine to induce dendritic cell maturation (34) and that of CPA to suppress regulatory T cells (Tregs) (30,31). Several daily, low-dose metronomic regimens have been shown to enhance anti-tumor immunity by selectively killing regulatory T suppressor cells and thereby restoring anti-tumor lymphocyte effector function, however, an increase in tumor NK cells was not established (31,35,36). In contrast, recruitment of immune cell infiltrates to the tumor microenvironment was shown here, and is likely to be critical to the major tumor regression responses that we observed. Moreover, our finding that large increases in tumor-associated NK cells occur not only in immune competent C57BL/6 mice but also in immunodeficient *scid* mice, which are devoid of Tregs, indicates that the NK cell response described here is both novel and mechanistically distinct from the relief of immune suppression by Tregs reported previously using daily low-dose metronomic schedules (31,35,36).

CPA given on a 6-day metronomic schedule may also potentiate anti-tumor adaptive immunity, as suggested by the increase in $CD8^+$ T cells through down regulation of iNOS (37). While iNOS regulation was not explored in the present study, we did observe a temporal delay in the recruitment of adaptive immune cytotoxic $CD8^+$ T cells to the regressing GL261 tumors. Perforin knock-out, which greatly impairs both innate and adaptive lymphocyte effector function (14), had a greater impact on tumor regression than antibody depletion of NK cells alone (Fig.6A), suggesting a role for adaptive $CD8^+$ T cells in the anti-tumor response to metronomic CPA.

The tumor regression responses reported here were robust, and were validated in three brain tumor xenografts models. Future studies will be required to extend these findings to other

tumor models, including orthotopic brain tumor models. Importantly, many orthotopic sites have endogenous innate immune cell populations, including the liver, which contains Kupffer and NK cells (38), and the brain, where microglia and NK cells can infiltrate tumors (39). Although the blood-brain barrier often impedes chemotherapeutic drug access to brain tumors, 4-hydroxy-CPA, the active metabolite of CPA, is membrane permeable and can cross the blood-brain barrier (40). Furthermore, brain tumors may be leaky, disrupting surrounding extracellular matrix and the blood-brain barrier itself (41).

Innate immune cell recruitment is shown to be a target for the inhibitory effects of several VEGF receptor-selective inhibitors on metronomic CPA-induced tumor regression. This finding has important implications for therapies combining chemotherapy, in particular metronomic chemotherapy, with VEGF receptor inhibitory anti-angiogenic drugs. While VEGF receptor signaling inhibitors can improve responses to some metronomic therapies (e.g., (29)), those studies typically employ daily low-dose metronomic drug treatment, which may be less effective at eliciting an anti-tumor immune response than the 6-day repeating metronomic CPA schedule used here (unpublished experiments). Furthermore, the suppression of innate immune cell recruitment by VEGF receptor inhibitors suggests that these drugs decrease immune surveillance, which could help explain the increases in metastatic incidence and progression recently linked to this class of anti-angiogenic agents (42). Supporting this hypothesis, metastatic infiltration of tumor cells in NOD/*scid* mice is increased by NK cell-depleting antibody, and metastasis is even more severe when tumor cells are grown in additionally immune-compromised NSG mice (43).

VEGF receptors, which are targeted by the three anti-angiogenic drugs used here, have been implicated in dendritic cell differentiation and are important for dendritic cell–endothelial cell cross-talk, trans-differentiation and tumor-associated macrophage infiltration (44). Endothelial cell VEGF signaling is also important for chemokine expression and secretion in proinflammatory responses (17), suggesting an additional mechanism whereby the inhibition of VEGF signaling could block innate immune cell recruitment. Indeed, in our models, the VEGF receptor inhibitor axitinib blocked induction of host (mouse) chemokines IL-12β and CXCL14 by metronomic CPA treatment. IL-12 is expressed and secreted by activated dendritic cells, neutrophils and macrophages and can activate anti-tumor NK cells and T cells (45), while CXCL14 stimulates activated NK cell migration (46). We observed that splenic NK cell reservoirs were decreased over time in metronomic CPA-treated *scid* mice, perhaps reflecting net immune cell migration out from the spleen and into the treated tumors. A corresponding decrease in splenic NK cell factors was not seen in immune competent C57BL/6 mice, which had higher basal levels of NK cells, both in spleen and in untreated tumors (Supplementary Fig.S4B).

The suppression of the innate immune response by VEGF receptor inhibitors reported here is likely due to the inhibition of VEGF signaling, rather than a secondary response to the associated loss of blood vessels required for immune cell trafficking into the tumor compartment, insofar as anti-angiogenic agents that decrease tumor vascularity without inhibiting VEGF signaling do not block metronomic CPA-stimulated anti-tumor innate immunity (unpublished data). Thus, inhibition of anti-tumor innate immunity is not a characteristic of anti-angiogenesis *per se*. Anti-angiogenic agents that target tumor endothelial cells without inhibition of VEGF receptor include the tubulin-targeting cytotoxic agent Oxi4053 and the cell cycle inhibitor TPN-470, both of which can enhance anti-tumor activity when combined with metronomic chemotherapy (3,47). In addition, TPN-470 inhibits both tumor metastases and primary tumor growth (48).

The empirical observation that a 6-day metronomic CPA schedule is optimal with regards to anti-tumor activity (3) could reflect the lifespan of host immune cells such as platelets,

which are first-line immune responders to tissue inflammation and damage and have a lifespan of 5–10-days (49). While other metronomic chemotherapy schedules, including daily, low-dose regimens, show anti-tumor activity (1), we suggest that an intermittent metronomic schedule, such as the every 6-day bolus CPA regimen used here, may be optimal with respect to activation of innate immunity: sufficiently frequent to repeatedly induce tumor cytotoxicity and inflammation and activate cytokine/chemokine attractants leading to an innate immune response, while at the same time sufficiently infrequent to minimize the killing of immune cells recruited to the tumor. While the metronomic dose of CPA used here is higher than metronomic dosages used in cancer patients, where daily metronomic dosing is most often used (1), our metronomic schedule (140 mg/kg CPA, every 6-days) is, in fact, slightly lower in total drug exposure to that of the low-dose, daily metronomic CPA regimen used in mouse models by others (25 mg/kg, daily, which corresponds to a total dose of 150 mg/kg every 6-days) to model metronomic dosing in the clinic (50). The exact dosing and metronomic timing requirements for an effective anti-tumor immune response can be expected to vary with the chemotherapeutic drug and are likely to benefit from efforts at optimization.

The precise nature of the cytotoxic damage, stress response and cytokine and chemokine signals required for metronomic CPA to elicit an anti-tumor immune response are unknown. The ability of metronomic CPA to induce such a response is likely to vary between tumors, insofar as the same metronomic CPA dose and schedule used in the present study did not elicit regression (51) or an innate immune response (unpublished data) in the case of PC-3 prostate tumor xenografts. Given the absence of immune cell involvement in the PC-3 model, it is not surprising that the combination of metronomic CPA with axitinib was more effective, rather than less effective against PC-3 tumors than metronomic CPA alone (51). Conceivably, an innate immune response leading to tumor regression may be achieved with PC-3 and other tumors by appropriate choice of drug, dose and metronomic schedule. Indeed, tumors derived from immortalized fibroblasts are regressed via an apoptosis-independent mechanism involving macrophages when CPA is given at 170 mg/kg on a 5-day repeating schedule (52), and regression of mammary MX-1, ovarian SK-OV-3, and neuroblastoma SK-NAS tumor xenografts is achieved when paclitaxel is given on various metronomic schedules (53). Further studies to investigate the involvement of NK and other immune cells in these tumor regression responses would be of interest.

Chemotherapeutic drugs elicit a variety of distinct types of DNA damage and activate different cellular stress responses, some of which are known to activate NK cells (54), which could be one mechanism whereby metronomic CPA activates an innate immune response. In U251 tumors grown in *scid* mice, we found that metronomic CPA induced tumor cell expression of MICB, a ligand for the innate immune cell activating-receptor NKG2D. Axitinib blocked this increase in MICB expression, further implicating tumor-cell specific expression of MICB in targeting of NK and other immune cells to the drug-treated tumors.

Supplementary Material

Refer to Web version on PubMed Central for supplementary material.

Acknowledgments

Supported by NIH grant CA049248 (to D.J.W.). We thank Chong-Sheng Chen for assistance with initial qPCR analysis.

References

1. Pasquier E, Kavallaris M, Andre N. Metronomic chemotherapy: new rationale for new directions. Nat Rev Clin Oncol. 2010; 7:455–465. [PubMed: 20531380]
2. Hanahan D, Bergers G, Bergsland E. Less is more, regularly: metronomic dosing of cytotoxic drugs can target tumor angiogenesis in mice. J Clin Invest. 2000; 105:1045–1047. [PubMed: 10772648]
3. Browder T, Butterfield CE, Kraling BM, Shi B, Marshall B, O'Reilly MS, et al. Antiangiogenic scheduling of chemotherapy improves efficacy against experimental drug-resistant cancer. Cancer Res. 2000; 60:1878–1886. [PubMed: 10766175]
4. Ma J, Waxman DJ. Modulation of the antitumor activity of metronomic cyclophosphamide by the angiogenesis inhibitor axitinib. Mol Cancer Ther. 2008; 7:79–89. [PubMed: 18202011]
5. Bocci G, Francia G, Man S, Lawler J, Kerbel RS. Thrombospondin 1, a mediator of the antiangiogenic effects of low-dose metronomic chemotherapy. Proc Natl Acad Sci U S A. 2003; 100:12917–12922. [PubMed: 14561896]
6. Ma J, Waxman DJ. Combination of antiangiogenesis with chemotherapy for more effective cancer treatment. Mol Cancer Ther. 2008; 7:3670–3684. [PubMed: 19074844]
7. Munoz R, Shaked Y, Bertolini F, Emmenegger U, Man S, Kerbel RS. Anti-angiogenic treatment of breast cancer using metronomic low-dose chemotherapy. Breast. 2005; 14:466–479. [PubMed: 16199161]
8. Cabebe E, Wakelee H. Role of anti-angiogenesis agents in treating NSCLC: focus on bevacizumab and VEGFR tyrosine kinase inhibitors. Curr Treat Options Oncol. 2007; 8:15–27. [PubMed: 17634832]
9. Verhoeff JJ, van Tellingen O, Claes A, Stalpers LJ, van Linde ME, Richel DJ, et al. Concerns about anti-angiogenic treatment in patients with glioblastoma multiforme. BMC Cancer. 2009; 9:444. [PubMed: 20015387]
10. Mah-Becherel MC, Ceraline J, Deplanque G, Chenard MP, Bergerat JP, Cazenave JP, et al. Anti-angiogenic effects of the thienopyridine SR 25989 in vitro and in vivo in a murine pulmonary metastasis model. Br J Cancer. 2002; 86:803–810. [PubMed: 11875746]
11. Krishnaswami S, Ly QP, Rothman VL, Tuszynski GP. Thrombospondin-1 promotes proliferative healing through stabilization of PDGF. J Surg Res. 2002; 107:124–130. [PubMed: 12384074]
12. Martin-Manso G, Galli S, Ridnour LA, Tsokos M, Wink DA, Roberts DD. Thrombospondin 1 promotes tumor macrophage recruitment and enhances tumor cell cytotoxicity of differentiated U937 cells. Cancer Res. 2008; 68:7090–7099. [PubMed: 18757424]
13. Pearson T, Greiner DL, Shultz LD. Humanized SCID mouse models for biomedical research. Curr Top Microbiol Immunol. 2008; 324:25–51. [PubMed: 18481451]
14. Kagi D, Ledermann B, Burki K, Seiler P, Odermatt B, Olsen KJ, et al. Cytotoxicity mediated by T cells and natural killer cells is greatly impaired in perforin-deficient mice. Nature. 1994; 369:31–37. [PubMed: 8164737]
15. Sozzani S, Rusnati M, Riboldi E, Mitola S, Presta M. Dendritic cell-endothelial cell cross-talk in angiogenesis. Trends Immunol. 2007; 28:385–392. [PubMed: 17692569]
16. Dineen SP, Lynn KD, Holloway SE, Miller AF, Sullivan JP, Shames DS, et al. Vascular endothelial growth factor receptor 2 mediates macrophage infiltration into orthotopic pancreatic tumors in mice. Cancer Res. 2008; 68:4340–4346. [PubMed: 18519694]
17. Boulday G, Haskova Z, Reinders ME, Pal S, Briscoe DM. Vascular endothelial growth factor-induced signaling pathways in endothelial cells that mediate overexpression of the chemokine IFN-gamma-inducible protein of 10 kDa in vitro and in vivo. J Immunol. 2006; 176:3098–3107. [PubMed: 16493069]
18. Katoh O, Tauchi H, Kawaishi K, Kimura A, Satow Y. Expression of the vascular endothelial growth factor (VEGF) receptor gene, KDR, in hematopoietic cells and inhibitory effect of VEGF on apoptotic cell death caused by ionizing radiation. Cancer Res. 1995; 55:5687–5692. [PubMed: 7585655]
19. Hu-Lowe DD, Zou HY, Grazzini ML, Hallin ME, Wickman GR, Amundson K, et al. Nonclinical antiangiogenesis and antitumor activities of axitinib (AG-013736), an oral, potent, and selective

inhibitor of vascular endothelial growth factor receptor tyrosine kinases 1, 2, 3. Clin Cancer Res. 2008; 14:7272–7283. [PubMed: 19010843]

20. Halin S, Rudolfsson SH, Doll JA, Crawford SE, Wikstrom P, Bergh A. Pigment epithelium-derived factor stimulates tumor macrophage recruitment and is downregulated by the prostate tumor microenvironment. Neoplasia. 2010; 12:336–345. [PubMed: 20360944]
21. Chu CY, Tseng J. Induction of Fas and Fas-ligand expression in plasmacytoma cells by a cytotoxic factor secreted by murine macrophages. J Biomed Sci. 2000; 7:58–63. [PubMed: 10644890]
22. Chavez-Galan L, Arenas-Del Angel MC, Zenteno E, Chavez R, Lascurain R. Cell death mechanisms induced by cytotoxic lymphocytes. Cell Mol Immunol. 2009; 6:15–25. [PubMed: 19254476]
23. Faure-Andre G, Vargas P, Yuseff MI, Heuze M, Diaz J, Lankar D, et al. Regulation of dendritic cell migration by CD74, the MHC class II-associated invariant chain. Science. 2008; 322:1705–1710. [PubMed: 19074353]
24. Bonmort M, Dalod M, Mignot G, Ullrich E, Chaput N, Zitvogel L. Killer dendritic cells: IKDC and the others. Curr Opin Immunol. 2008; 20:558–565. [PubMed: 18554881]
25. Balkwill F. Cancer and the chemokine network. Nat Rev Cancer. 2004; 4:540–550. [PubMed: 15229479]
26. Champsaur M, Lanier LL. Effect of NKG2D ligand expression on host immune responses. Immunol Rev. 2010; 235:267–285. [PubMed: 20536569]
27. Wedge SR, Kendrew J, Hennequin LF, Valentine PJ, Barry ST, Brave SR, et al. AZD2171: a highly potent, orally bioavailable, vascular endothelial growth factor receptor-2 tyrosine kinase inhibitor for the treatment of cancer. Cancer Res. 2005; 65:4389–4400. [PubMed: 15899831]
28. Zou HY, Qiuhua Li MG, Dillon R, Amundson K, Acena A, Wickman G, et al. Proc Amer Assoc Cancer Res. 2004; 45
29. Garcia AA, Hirte H, Fleming G, Yang D, Tsao-Wei DD, Roman L, et al. Phase II clinical trial of bevacizumab and low-dose metronomic oral cyclophosphamide in recurrent ovarian cancer: a trial of the California, Chicago, and Princess Margaret Hospital phase II consortia. J Clin Oncol. 2008; 26:76–82. [PubMed: 18165643]
30. Zitvogel L, Apetoh L, Ghiringhelli F, Andre F, Tesniere A, Kroemer G. The anticancer immune response: indispensable for therapeutic success? J Clin Invest. 2008; 118:1991–2001. [PubMed: 18523649]
31. Ghiringhelli F, Menard C, Puig PE, Ladoire S, Roux S, Martin F, et al. Metronomic cyclophosphamide regimen selectively depletes CD4+CD25+ regulatory T cells and restores T and NK effector functions in end stage cancer patients. Cancer Immunol Immunother. 2007; 56:641–648. [PubMed: 16960692]
32. Habu S, Fukui H, Shimamura K, Kasai M, Nagai Y, Okumura K, et al. In vivo effects of anti-asialo GM1. I. Reduction of NK activity and enhancement of transplanted tumor growth in nude mice. J Immunol. 1981; 127:34–38. [PubMed: 7240748]
33. Zitvogel L, Apetoh L, Ghiringhelli F, Kroemer G. Immunological aspects of cancer chemotherapy. Nat Rev Immunol. 2008; 8:59–73. [PubMed: 18097448]
34. Tanaka H, Matsushima H, Nishibu A, Clausen BE, Takashima A. Dual therapeutic efficacy of vinblastine as a unique chemotherapeutic agent capable of inducing dendritic cell maturation. Cancer Res. 2009; 69:6987–6994. [PubMed: 19706755]
35. Banissi C, Ghiringhelli F, Chen L, Carpentier AF. Treg depletion with a low-dose metronomic temozolomide regimen in a rat glioma model. Cancer Immunol Immunother. 2009; 58:1627–1634. [PubMed: 19221744]
36. Chen CA, Ho CM, Chang MC, Sun WZ, Chen YL, Chiang YC, et al. Metronomic chemotherapy enhances antitumor effects of cancer vaccine by depleting regulatory T lymphocytes and inhibiting tumor angiogenesis. Mol Ther. 2010; 18:1233–1243. [PubMed: 20372107]
37. Loeffler M, Kruger JA, Reisfeld RA. Immunostimulatory effects of low-dose cyclophosphamide are controlled by inducible nitric oxide synthase. Cancer Res. 2005; 65:5027–5030. [PubMed: 15958544]

38. Seki S, Habu Y, Kawamura T, Takeda K, Dobashi H, Ohkawa T, et al. The liver as a crucial organ in the first line of host defense: the roles of Kupffer cells, natural killer (NK) cells and NK1.1 Ag+ T cells in T helper 1 immune responses. Immunol Rev. 2000; 174:35–46. [PubMed: 10807505]
39. Yang I, Han SJ, Sughrue ME, Tihan T, Parsa AT. Immune cell infiltrate differences in pilocytic astrocytoma and glioblastoma: evidence of distinct immunological microenvironments that reflect tumor biology. J Neurosurg. 2011
40. Motl S, Zhuang Y, Waters CM, Stewart CF. Pharmacokinetic considerations in the treatment of CNS tumours. Clin Pharmacokinet. 2006; 45:871–903. [PubMed: 16928151]
41. Kemper EM, Leenders W, Kusters B, Lyons S, Buckle T, Heerschap A, et al. Development of luciferase tagged brain tumour models in mice for chemotherapy intervention studies. Eur J Cancer. 2006; 42:3294–3303. [PubMed: 17027258]
42. Loges S, Mazzone M, Hohensinner P, Carmeliet P. Silencing or fueling metastasis with VEGF inhibitors: antiangiogenesis revisited. Cancer Cell. 2009; 15:167–170. [PubMed: 19249675]
43. Dewan MZ, Terunuma H, Ahmed S, Ohba K, Takada M, Tanaka Y, et al. Natural killer cells in breast cancer cell growth and metastasis in SCID mice. Biomed Pharmacother. 2005; 59 Suppl 2:S375–S379. [PubMed: 16507413]
44. Johnson B, Osada T, Clay T, Lyerly H, Morse M. Physiology and therapeutics of vascular endothelial growth factor in tumor immunosuppression. Curr Mol Med. 2009; 9:702–707. [PubMed: 19689297]
45. Trinchieri G. Interleukin-12 and the regulation of innate resistance and adaptive immunity. Nat Rev Immunol. 2003; 3:133–146. [PubMed: 12563297]
46. Starnes T, Rasila KK, Robertson MJ, Brahmi Z, Dahl R, Christopherson K, et al. The chemokine CXCL14 (BRAK) stimulates activated NK cell migration: implications for the downregulation of CXCL14 in malignancy. Exp Hematol. 2006; 34:1101–1105. [PubMed: 16863917]
47. Daenen LG, Shaked Y, Man S, Xu P, Voest EE, Hoffman RM, et al. Low-dose metronomic cyclophosphamide combined with vascular disrupting therapy induces potent antitumor activity in preclinical human tumor xenograft models. Mol Cancer Ther. 2009; 8:2872–2881. [PubMed: 19825805]
48. Yanase T, Tamura M, Fujita K, Kodama S, Tanaka K. Inhibitory effect of angiogenesis inhibitor TNP-470 on tumor growth and metastasis of human cell lines in vitro and in vivo. Cancer Res. 1993; 53:2566–2570. [PubMed: 7684319]
49. Najean Y, Ardaillou N, Dresch C. Platelet lifespan. Annu Rev Med. 1969; 20:47–62. [PubMed: 4894508]
50. Man S, Bocci G, Francia G, Green SK, Jothy S, Hanahan D, et al. Antitumor effects in mice of low-dose (metronomic) cyclophosphamide administered continuously through the drinking water. Cancer Res. 2002; 62:2731–2735. [PubMed: 12019144]
51. Ma J, Waxman DJ. Dominant effect of antiangiogenesis in combination therapy involving cyclophosphamide and axitinib. Clin Cancer Res. 2009; 15:578–588. [PubMed: 19147763]
52. Guerriero JL, Ditsworth D, Fan Y, Zhao F, Crawford HC, Zong WX. Chemotherapy induces tumor clearance independent of apoptosis. Cancer Res. 2008; 68:9595–9600. [PubMed: 19047135]
53. Chou TC, Zhang X, Zhong ZY, Li Y, Feng L, Eng S, et al. Therapeutic effect against human xenograft tumors in nude mice by the third generation microtubule stabilizing epothilones. Proc Natl Acad Sci U S A. 2008; 105:13157–13162. [PubMed: 18755900]
54. Raulet DH, Guerra N. Oncogenic stress sensed by the immune system: role of natural killer cell receptors. Nat Rev Immunol. 2009; 9:568–580. [PubMed: 19629084]

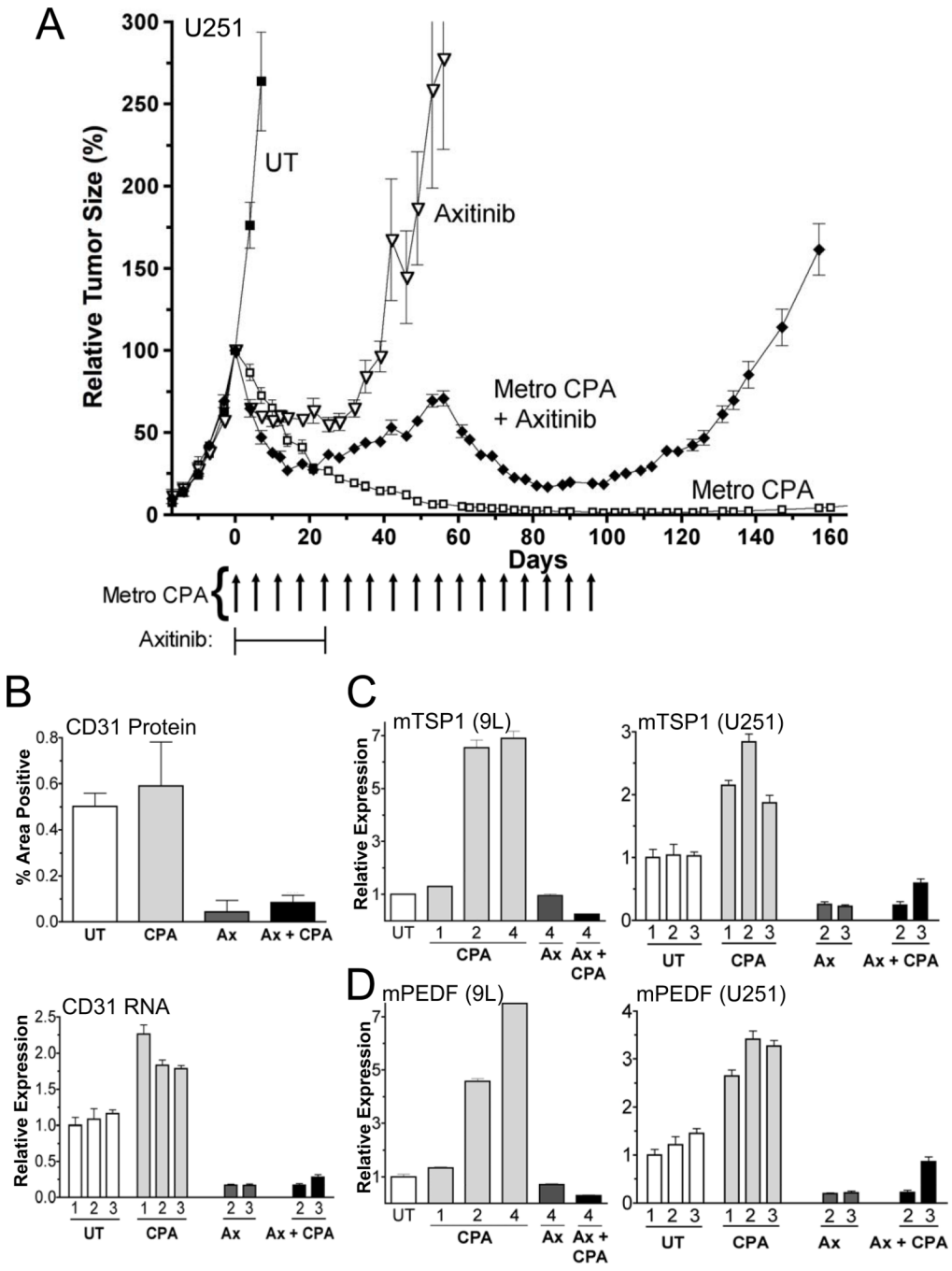

Figure 1. Metronomic CPA-induced regression of U251 tumors and inhibitory effects of the VEGF receptor-selective inhibitor axitinib

(A) Human U251 glioblastoma xenografts grown in *scid* mice were untreated (UT) or were treated with metronomic CPA (140mg/kg i.p., every 6-days for 17-cycles; arrows along x-axis), daily axitinib (Ax, 25mg/kg, i.p. daily for 24-days), or metronomic CPA in combination with daily axitinib. Tumor volumes were normalized to 100% on the day of first drug treatment (day-0), when group averages reached ~500mm^3 (n=12 tumors/group). Tumors were inoculated 32-days prior to the start of drug treatment. (B) U251 tumors treated as indicated were immunohistochemically stained for the endothelial cell marker CD31 protein (*top*; 12-days after initiating drug treatment; **, p<0.001 compared to UT

control group) or assayed by qPCR for CD31 RNA (*bottom*; 6-days after the 1st, 2nd and 3rd CPA treatments, as marked). CD31 immunohistochemical staining was quantified as described under Materials and Methods. qPCR analysis of host (m, mouse) TSP1 (C) and PEDF expression (D) in 9L rat (*left*) and U251 human (*right*) tumors grown in *scid* mice, treated as in panel A and isolated 6-days after the indicated number of CPA injections. For each comparison, qPCR data were normalized to the first untreated (UT) tumor group, whose relative RNA level was set to 1. Where indicated ('m'), qPCR analysis was carried out using mouse (host)-specific primers. Bars, mean ±SE for n=5–6 tumors/group. See also Fig.S1.

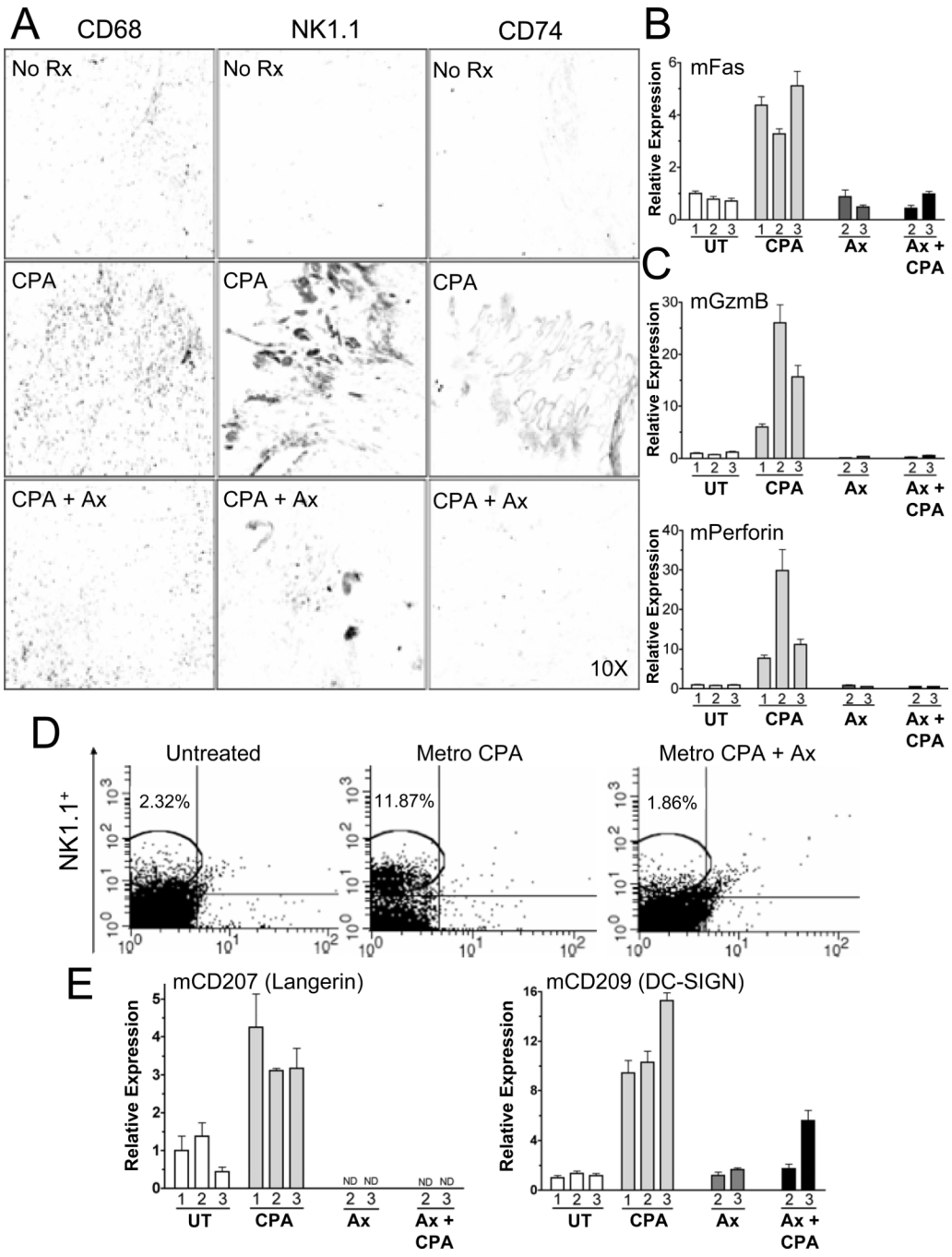

Figure 2. Metronomic CPA induces, and axitinib blocks, recruitment of macrophages, NK cells and dendritic cells to U251 tumors

(A) Immunostaining of macrophage (*left*), NK cell (*middle*), and dendritic cell markers (*right*) in U251 tumors, untreated (*no Rx*) or treated with metronomic CPA±axitinib, and excised on treatment day-12, as in Fig.1A. Representative images are shown with signal intensities equivalent to group mean ImageJ quantification data (i.e., Fig.S2C). (B,C,E), Expression of the indicated host factors (m, mouse) in U251 tumors 6-days after the 1st, 2nd or 3rd metronomic CPA injection±axitinib treatment, as marked. qPCR data were normalized to the first untreated (UT) tumor group, whose relative RNA level was set to 1. Bars, mean±SE for n=5–6 tumors/group. (D) FACS analysis of NK1.1+ cells (%) in single-

cell suspensions prepared from untreated and CPA-treated and/or axitinib-treated 9L tumors grown in *scid* mice. IgG background control, 0.54%. CD49b (no change with treatment) was the marker along the x-axis. See also Fig.S2.

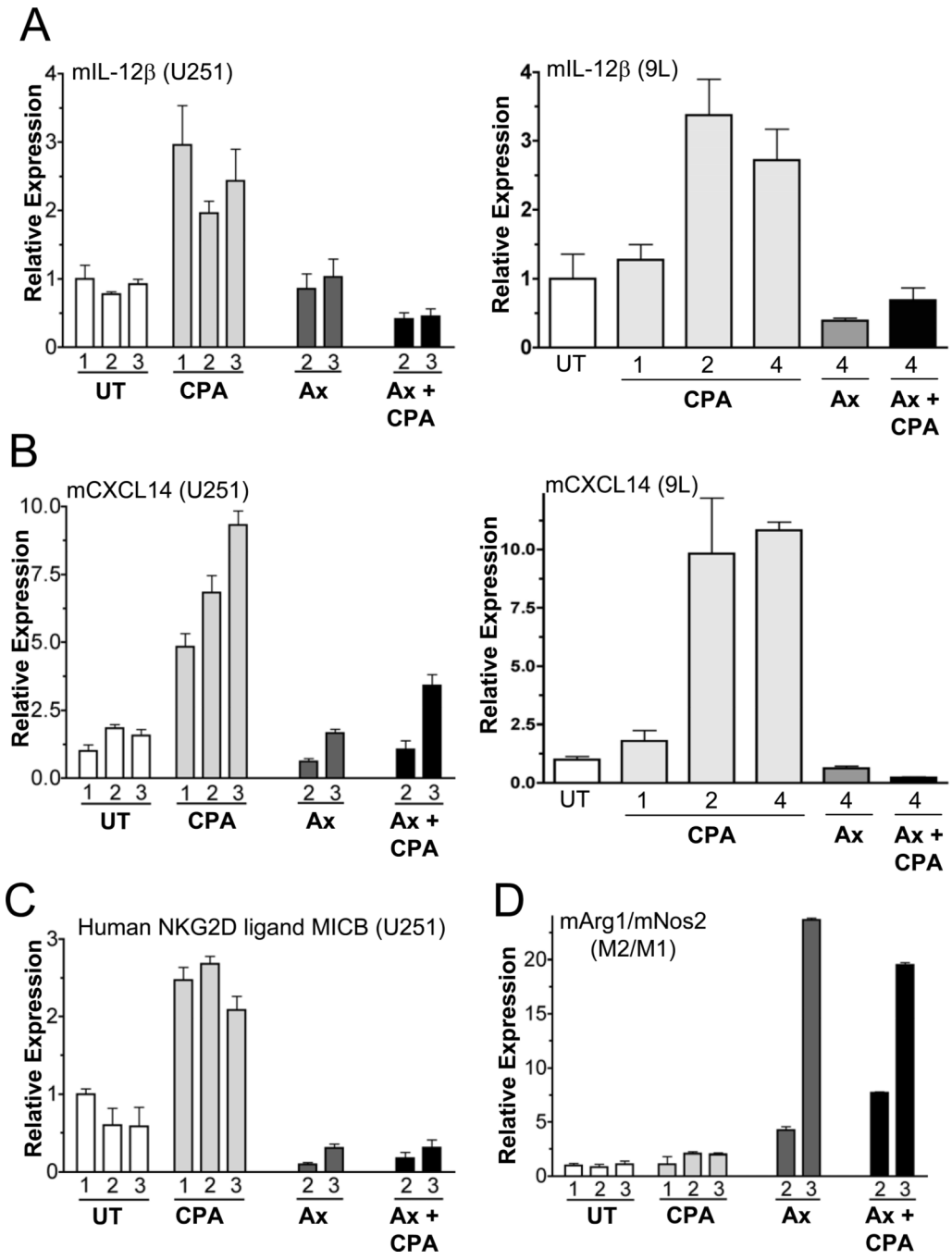

Figure 3. Axitinib blocks cytokine, chemokine and other responses to metronomic CPA

qPCR analysis of host (m, mouse) macrophage-associated interleukin-12β (A), NK cell-associated CXCL14 (B), and human tumor cell-specific MICB, an activating ligand for the immune cell receptor NKG2D (C), in metronomic CPA-treated U251 and 9L tumor xenografts grown in *scid* mice. (D) Axtinib, both alone and in combination with metronomic CPA, shifted the tumor infiltrating macrophage subpopulations to the pro-tumor M2 subtype, as indicated by the ratio of pro-tumor (M2) macrophage marker (arginase-1; *Arg1*) to anti-tumor (M1) macrophage marker (iNOS; *Nos2*) expression in the same set of U251 tumors. qPCR data were normalized to the first untreated (UT) tumor group, whose relative RNA level was set to 1. Bars, mean±SE for n=5–6 tumors/group.

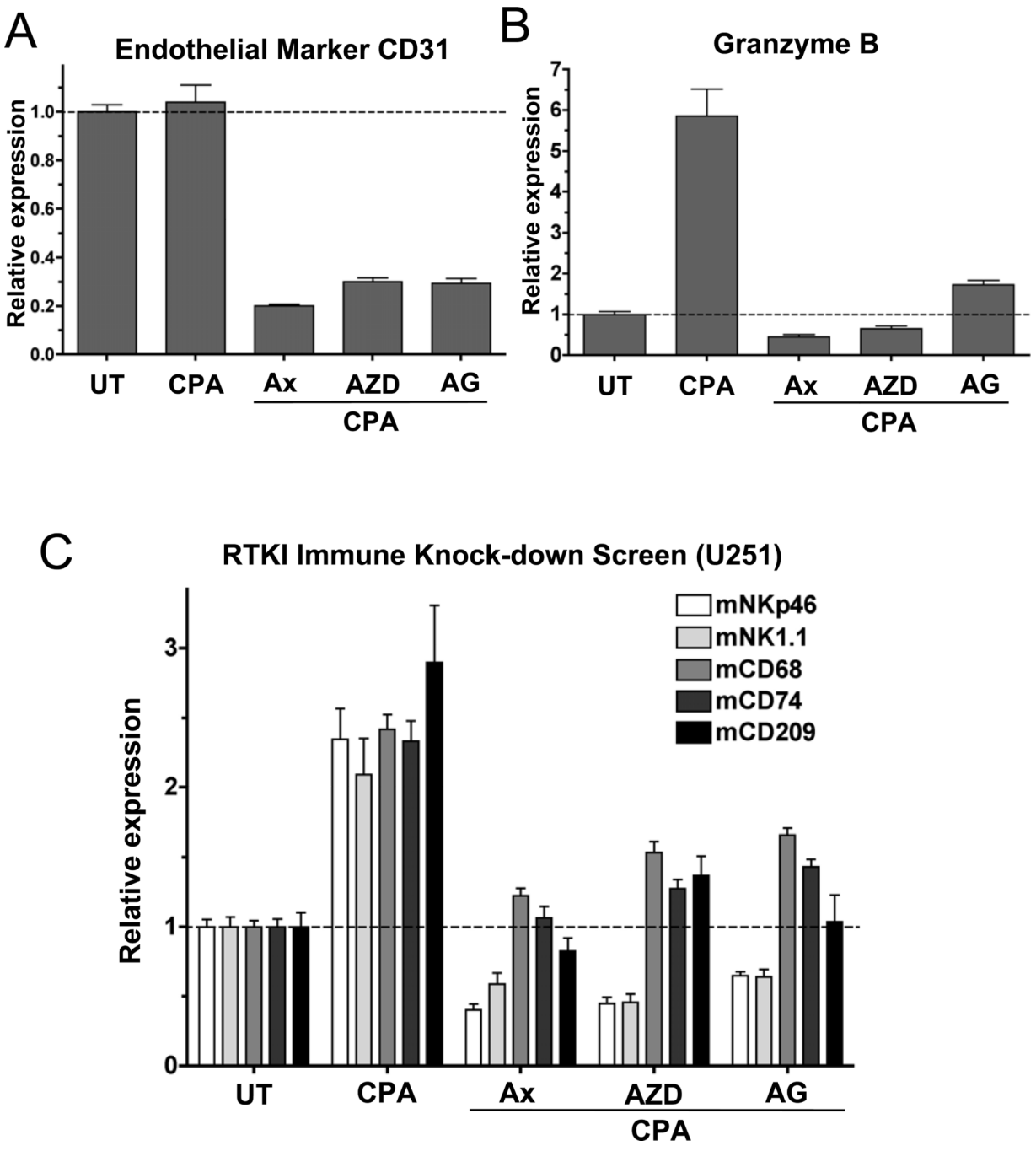

Figure 4. Immunosuppressive effects of VEGF receptor tyrosine kinase inhibitors

U251 tumors grown in *scid* mice were treated with metronomic CPA given alone or in combination with daily axitinib (Ax, 25mg/kg day, i.p.), cediranib (AZD, AZD2171; 5mg/kg/day, i.p.), or AG-028262 (AG, 25mg/kg day, i.p.). Each anti-angiogenic drug was given daily for 18-days prior to the analysis shown. (A) VEGF receptor-selective inhibitors suppress tumor angiogenesis (CD31 expression) and (B) block metronomic CPA induction of granzyme B in U251 tumors grown in *scid* mice, as compared to untreated (UT) controls, determined 6-days after the 3rd CPA injection (day-18). (C) VEGF receptor-selective inhibitors block metronomic CPA-induced immune recruitment in U251 tumors, as determined by qPCR analysis of NK cell markers NKp46 and NK1.1, macrophage marker

CD68, and dendritic cell markers CD74 and CD209. qPCR data were normalized to untreated (UT), whose relative RNA level was set to 1. Bars, mean±SE for n=5–6 tumors/group.

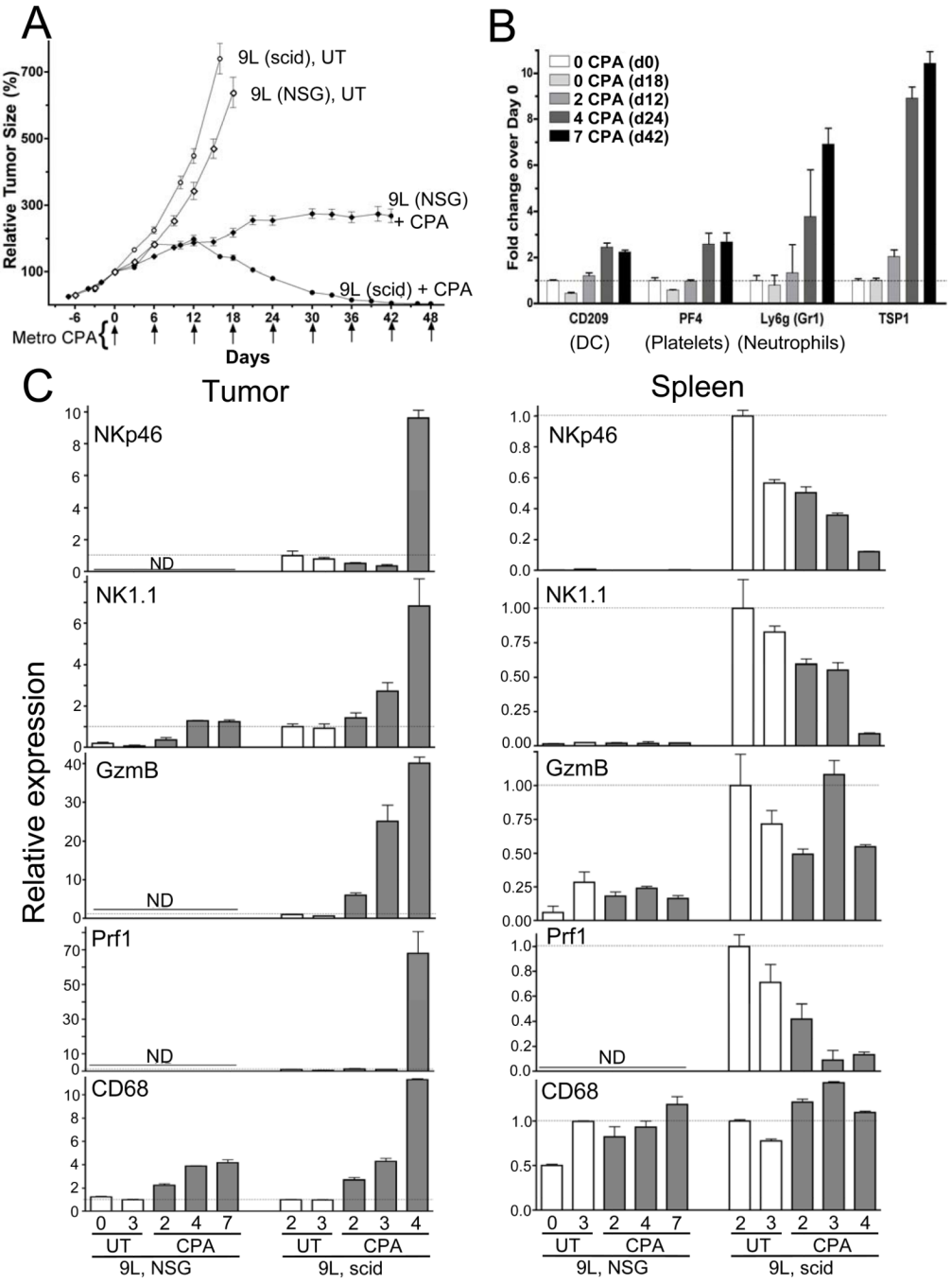

Figure 5. Anti-tumor activity of metronomic CPA in NSG mice (adaptive and innate immune-compromised)

(A) 9L tumor growth profiles in NSG and scid mice, with tumors implanted 14-days prior to the first CPA treatment (n=12 tumors/group). (B) qPCR of the indicated factors in 9L tumors ± metronomic CPA-treatment and isolated on day-0 or 6-days after the 2nd, 4th, or 7th treatment cycle (days 12–42, as marked). Bars, mean±SE for n=5–6 tumors/group. (C) qPCR of the indicated factors in 9L tumors (*left*) and spleens (*right*) ± metronomic CPA-treatment isolated from NSG or *scid* mice on day-0 or 6-days after the 2nd, 4th, or 7th treatment cycle. For each comparison, qPCR data were normalized to the first untreated (UT) *scid* tumor or spleen group, whose relative RNA level was set to 1. The absence of

NKp46, granzyme B (GzmB) and perforin (Prf1) reflects the NK cell deficiency of NSG mice. See Supplemental Materials for C_T values determined by qPCR. White bars, untreated tumor and spleen samples; shaded bars, treated samples. Bars, mean ±SD for tumor (n=4–6) and spleen (n=2–3) pools. DC, dendritic cell; ND, not detectable.

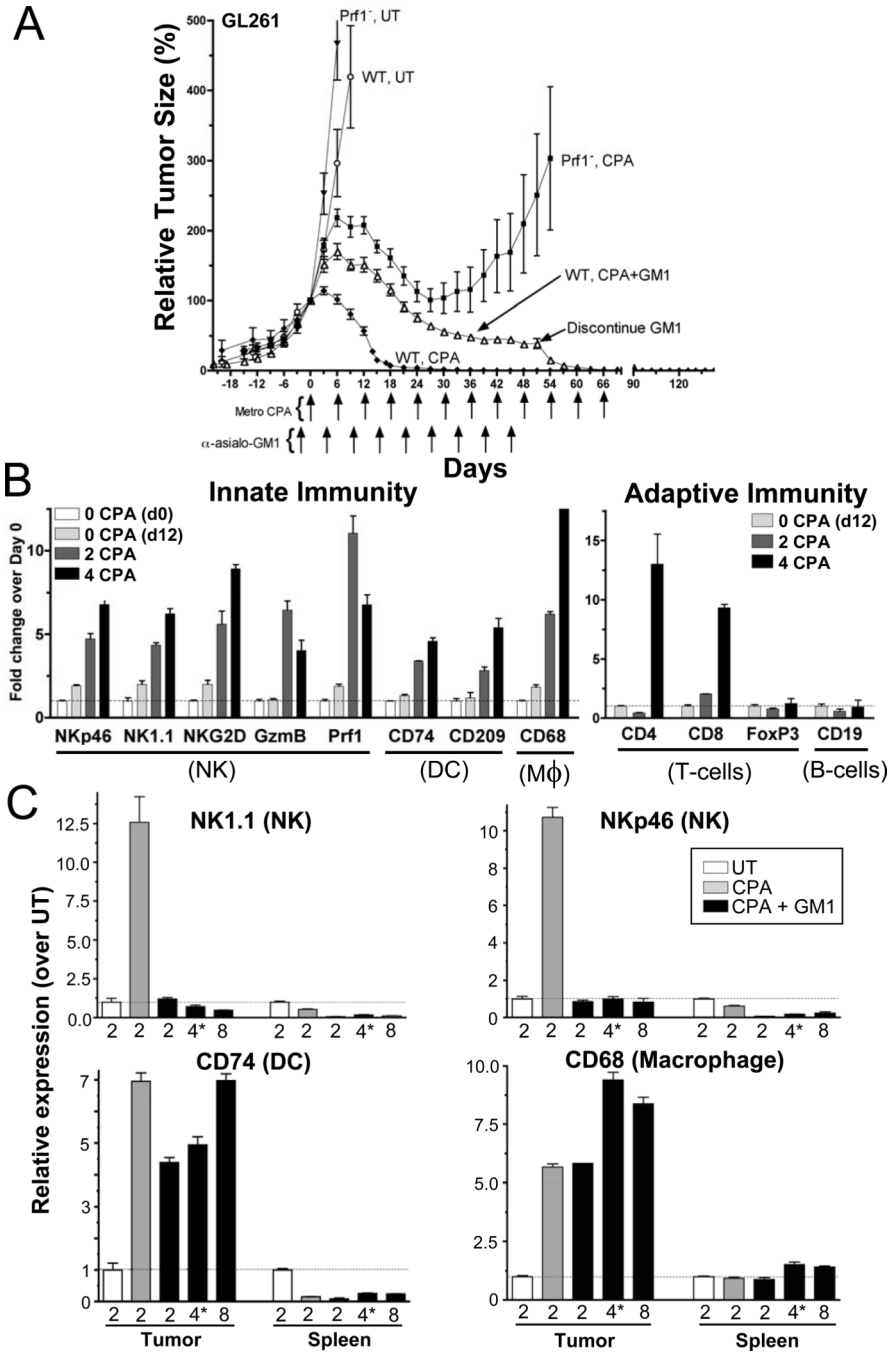

Figure 6. Response of GL261 tumors to metronomic CPA in C57BL/6 wild-type (WT) and perforin knock-out mice (Prf1¯) and impact of NK cell depletion

(A) Tumor growth profiles (n=12 tumors/group) showing metronomic CPA-induced regression in WT mice; regression is delayed and incomplete in Prf1⁻ mice, and also following NK cell depletion in WT mice (anti-asialo-GM1 antibody given every 6-days beginning 3-days prior to the first CPA injection; arrows). Anti-asialo-GM1 was discontinued on day-51; CPA was terminated on days 60 and 54 in WT and Prf1⁻ mice, respectively. Tumors were inoculated 28-days prior to the first CPA treatment (day-0). (B) qPCR analysis of mouse (host cell) innate and adaptive immune factors in untreated GL261 tumors collected on days 0 and/or 12, and in tumors 6-days after either 2 or 4 CPA treatment

cycles, as marked. Mϕ, macrophage; DC, dendritic cell. Genes assayed include those shown in earlier Figures, as well as markers for helper (CD4) and cytotoxic effector (CD8) T-cells and T-regulatory cells (FoxP3) and B-cells (CD19). The strong increase in CD4- and CD8-marked T-cells was delayed when compared to the innate immune cells and the onset of tumor regression. Data were normalized to the first untreated (UT) tumor group, whose relative RNA level was set to 1. Bars, mean ±SE for n=5–6 tumors/group. C) qPCR analysis showing depletion of NK cells by anti-asialo-GM1; tumors and spleens from mice in (A) were collected 6-days after 2 CPA cycles (i.e., day-12) without anti-asialo-GM1 (UT) or 6-days after the 2^{nd}, 3-days (*) after the 4^{th}, and 6-days after the 8^{th} CPA cycle with anti-asialo-GM1 treatment. Anti-asialo-GM1 depleted NK cells from tumors and spleens and blocked their recruitment into metronomic CPA-treated tumors. The partial regression seen with anti-asialo-GM1 in (A) may result from the unimpeded recruitment of dendritic cells and macrophages, seen in the lower panels of C. qPCR data were normalized to untreated (UT), whose relative RNA level was set to 1. Bars, mean ±SE for n=5–6 tumors/group. See also Fig.S3.

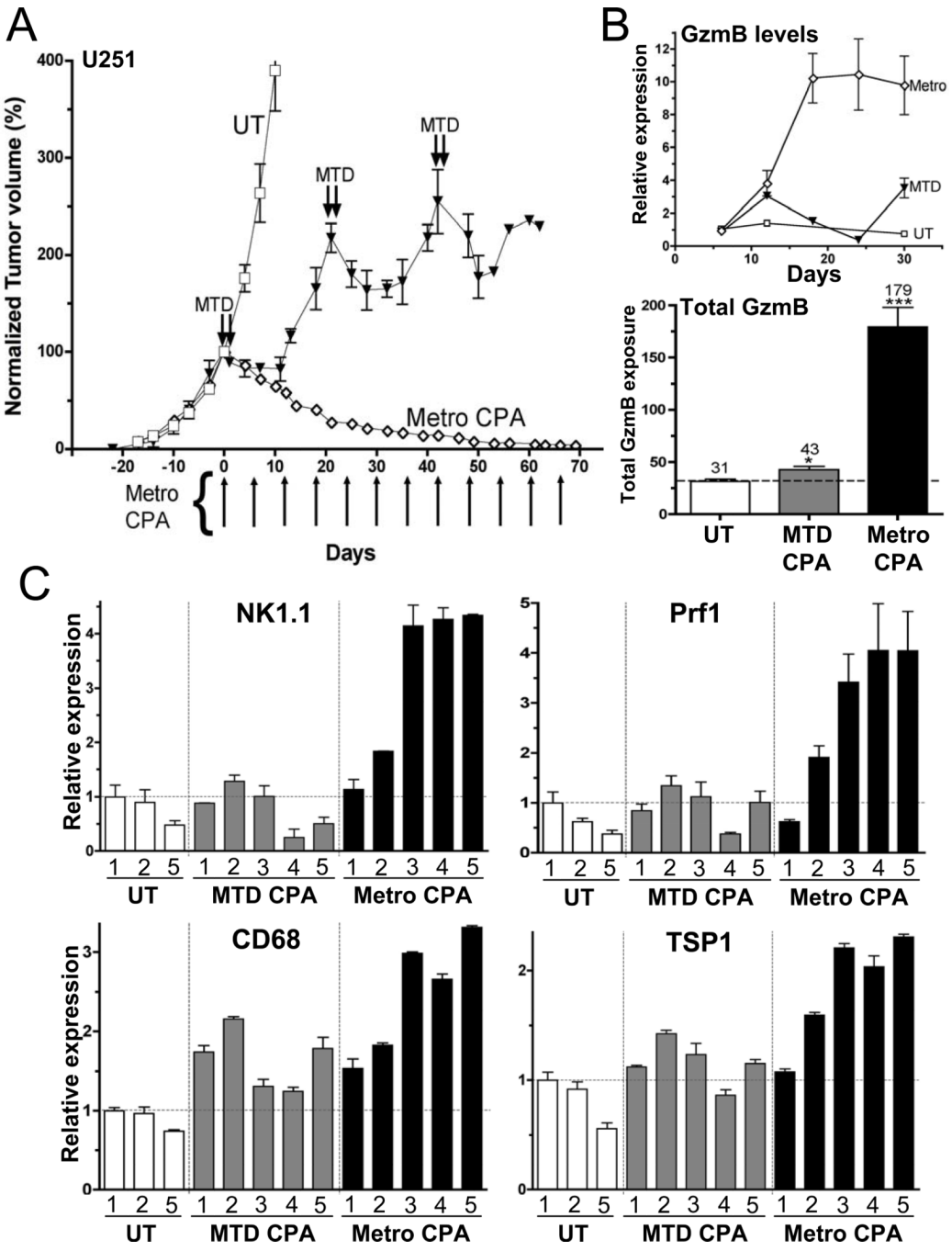

Figure 7. Response of U251 tumors to metronomic versus MTD CPA

(A) Growth curves for U251 tumor in *scid* mice administered either metronomic or MTD CPA (n=12 tumors/group). Untreated (UT) and metronomic CPA-treated U251 curves are the same as in Fig.1A. (B) U251 tumors isolated at the indicated times after initiating CPA treatment as in (A) were analyzed for granzyme B expression (*top*) and total (integrated) granzyme B RNA levels from day-0 through day-30, which increased 1.4-fold (from 31 to 43 arbitrary units) (MTD CPA) versus 5.8-fold (from 31 to 179 arbitrary units) (metronomic CPA) (*bottom*). *, $p<0.05$; ***, $p<0.0001$ versus UT tumors. (C) qPCR analysis of marker genes in U251 tumors collected after the indicated number of 6-day schedule intervals (1=day 6 after first CPA treatment, 5=day 30). Data were normalized to the first untreated

(UT) tumor group, whose relative RNA level was set to 1. Bars, mean ±SE for n =5–6 tumors/group.